



# Polarization-selective excitation of plasmonic resonances in silver nanocube random arrays by optical fiber cladding mode evanescent fields†

Cite this: *RSC Adv.*, 2014, 4, 19725Anatoli Ianoou,<sup>\*a</sup> Mitchell Robson,<sup>‡ab</sup> Vladislav Pripotnev<sup>§a</sup> and Jacques Albert<sup>b</sup>

Near-field scanning optical microscopy was used in collection mode to examine the optical field distribution on the surface of tilted fiber Bragg gratings (TFBGs) coated with a layer of randomly spaced silver nanocubes. The nanocubes disturb the periodic pattern of the near field visible light distribution arising from counterpropagating cladding modes excited by the TFBG. Spots with more than two orders of magnitude enhancement of the near field light intensity were observed around the nanocubes, as well as an average enhancement over the whole surface of about an order of magnitude relative to uncoated fibers. The near field speckle pattern associated with nanocubes showed a 180-degree periodicity with respect to the linear polarization of the input excitation light launched in the fiber core. The observed phenomena are explained in terms of the plasmonic properties of silver nanocubes. The enhancement factors measured here explain previously observed improvements in the performance of metal nanoparticle coated TFBG devices in sensing and as sources of light for surface-enhanced spectroscopy.

Received 27th January 2014

Accepted 11th April 2014

DOI: 10.1039/c4ra02770a

[www.rsc.org/advances](http://www.rsc.org/advances)

## Introduction

Localized (nanometer scale) and strong (several orders of magnitude) enhancement of electric field provided by plasmonic nanostructures, for example gold or silver nanoparticles, helps amplify various physical and chemical processes and phenomena. As a result, today such nanomaterials find use in numerous applications including surface-enhanced optical techniques,<sup>1,2</sup> photovoltaics<sup>3</sup> and photo-catalysis.<sup>4,5</sup> Different sensing methods and platforms can benefit particularly from such enhancement, leading often to a single molecule detection limits.<sup>6–8</sup> One sensing platform that was proposed recently relies on refractive index sensitivity of photonic modes in tilted fiber Bragg grating (TFBG).<sup>9</sup> Extremely narrow half-width of peaks in transmission spectra measured with such platform enables very small changes of the surroundings refractive index to be detected.<sup>9</sup> Yet, further optimization and improvement of the platform is possible through coupling of the TFBG with high

refractive index dielectric or plasmonic nanomaterials.<sup>4–11</sup> For example, in our recent studies of TFBG over-coated with a plasmonic layer we observed an order of magnitude enhancement of the refractive index sensitivity,<sup>12</sup> as well as an improvement in the detection limit for the avidin–biotin pair by several orders of magnitude.<sup>13</sup> In addition, these fiber based devices can be used for efficient excitation of optical signals,

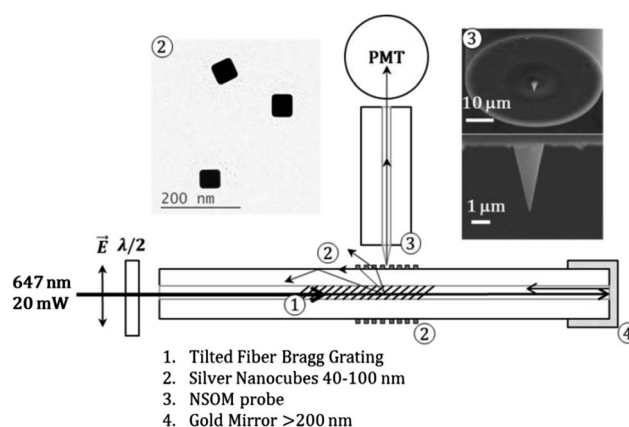


**Fig. 1** Experimental setup used. A tilted fiber Bragg grating (TFBG, 1) containing fiber was mounted on a glass slide and positioned in the NSOM instrument. Silver nanocubes (2) with edge length 40–100 nm and plasmon resonances between 350 and 700 nm were deposited on half of the TFBG length. NSOM probes (3) fabricated by chemical etching were used to collect the near-field signal further detected with a photomultiplier tube (PMT). Excitation was provided by a continuous wave ion laser at 647 nm and 20 mW. A half-wave plate was used to control polarization.

<sup>a</sup>Department of Chemistry, Carleton University, 1125 Colonel By Dr., Ottawa, ON, Canada. E-mail: [anatoli\\_ianoou@carleton.ca](mailto:anatoli_ianoou@carleton.ca); Fax: +1 (613)-520-3749; Tel: +1 (613)-520-2600 ext. 6043

<sup>b</sup>Department of Electronics, Carleton University, 1125 Colonel By Dr., Ottawa, ON, Canada

† Electronic supplementary information (ESI) available: NSOM and topography images for various polarizations of excitations light, TEM images. See DOI: 10.1039/c4ra02770a

‡ Present address: Faculty of Engineering, McMaster University, Hamilton, ON, Canada.

§ Present address: Faculty of Engineering, University of Waterloo, Waterloo, ON, Canada.

such as in surface enhanced Raman scattering.<sup>14</sup> The phenomena mentioned rely on the enhancement of the interrogating light intensity near the surface of metal nanostructure because of plasmonic excitations. In the case of TFBG devices, it is the evanescent field component of optical modes guided by the cladding that is enhanced by plasmonic nanostructures. Yet, although such explanation of the observed fiber sensor improvements is reasonable no supporting experimental evidence has been provided so far. To address the issue, in this work near-field scanning optical microscopy (NSOM) was used to probe directly the intensity and spatial distribution of the plasmon-enhanced optical near fields of the evanescent modes on the surface of TFBG devices coated with silver nanocubes (Fig. 1).

## Results and discussion

### Description of experimental platform

**TFBG.** TFBG provides a way to excite a large number of waveguide modes in the cladding of the optical fiber with the ability to probe directly the fiber-surroundings interface.<sup>9</sup> By controlling the polarization of the light launched in the fiber, the modes excited by the TFBG can be selected to have predominantly azimuthal or predominantly radial electric field orientation at the cladding boundary,<sup>15</sup> and hence across any coating deposited on the fiber. While some of the modes are radiative in nature and exit the fiber at a particular angle dependent on the grating period as well as the incident wavelength, many modes excited remain guided with the majority of the mode energy confined inside the fiber. In order to make use of such guided modes (either excite the signal from a sample near the fiber surface (analogous to total internal reflection or dark field microscopy) or to probe the changes in the local environment due to sensing events, it is necessary to maximize the mode fraction protruding outside the fiber—essentially to extract it from the fiber.

To achieve this goal, local perturbations of the refractive index just outside the fiber can be used, such as thin high index coatings,<sup>10,11</sup> but the largest improvements are obtained when metal coatings allowing the excitation of surface wave plasmons are used.<sup>9</sup>

In particular, even sparse layers of metal nanoparticles have led to significant sensitivity enhancements.<sup>12</sup> The effect of nanoparticles on light extraction from optical fibers can be seen even for light coupled to radiation modes by TFBGs.<sup>16,17</sup> The far field image shown in Fig. 2 has the left hand side of the TFBG coated with silver nanocubes and the right hand side left bare.

**Nanocubes.** Nanocubes of 40–100 nm edge length (Fig. 1, inset 2) were chosen in the study to provide enhancement of the photonics modes outside of the fiber. Unlike spherical particles of the same size, nanocubes allow excitation of a larger number of localized surface plasmon resonances.<sup>18–20</sup> In addition, for supported silver nanocubes plasmonic resonances can be represented in terms of hybrid modes: lower energy hybrid dipole (D) and higher energy quadrupole (Q).<sup>21</sup> Of particular importance is the fact that the hybrid dipolar resonance is associated primarily with oscillations of electrons at the nanocube facet

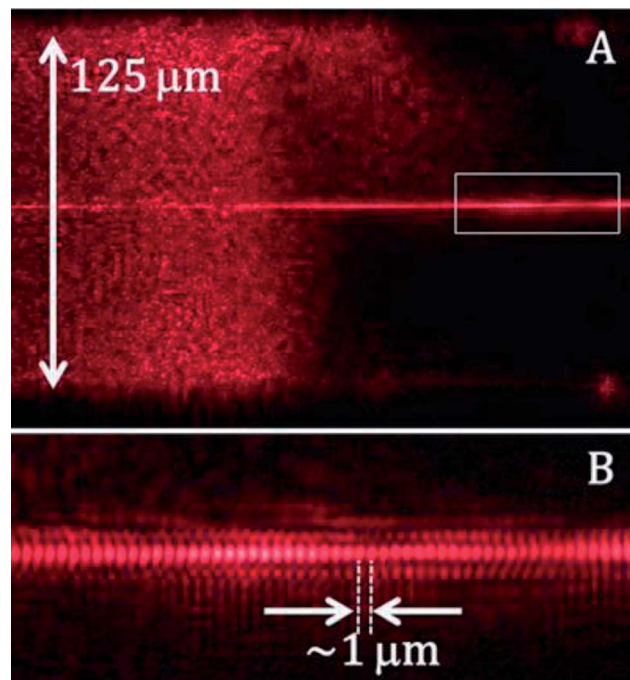


Fig. 2 Far field light microscopy image of light diffracted by a tilted fiber Bragg grating at a wavelength of 647 nm. (A) Light distribution on the TFBG with the left half of the grating covered with silver nanocubes. (B) A zoom of the area indicated in panel A showing the period of  $\sim 1$  micrometer in the diffracted light measured in the far field.

close to the supporting surface. Therefore, such dipolar resonance can be excited by the stronger electric field of the evanescent component of a cladding guided mode leading to potentially more efficient light extraction from the fiber. Additionally, a strong polarization dependence of the nanocube extinction spectra,<sup>22</sup> and particularly of the Q resonance can be investigated using the cladding mode polarization selection features of the TFBG.

The radiation (far field) pattern from the uncoated part of the fiber is periodic with a period near 1 micrometer (Fig. 2). The far field period results from the interference between pair of nearly collinear radiated beams emitted by the interaction between the incident core-guided light and the grating. The fact that two beams directions are radiated comes from very minute inaccuracies in the TFBG writing process that result in the superposition of nearly identical gratings in the fiber core with periods corresponding to radiative mode couplings.<sup>21</sup> The coated TFBG however shows a completely different intensity distribution with essentially the entire circumference of the fiber brightly illuminated due to scattering of the radiated light by the nanocubes (Fig. 2A, left side).

**NSOM.** The near field properties of the bare and coated TFBGs were measured with the collection mode NSOM (also known as photon scanning tunneling microscopy).<sup>23</sup> Unlike the far field microscopy NSOM allows collecting not only the radiative modes coming out of the TFBG but also to observe directly the evanescent tail of guided modes extending outside of the cladding. We use high efficiency NSOM probes prepared by a

chemical etching process<sup>24</sup> in shear force mode to maximize the collection of the near field signal. To eliminate possible plasmonic artifacts no metal coating combined with focused ion beam milling was applied to form the aperture.<sup>24,25</sup> At the same time, although the absence of coating on the probe reduces the signal to noise (near to far field) ratio, the tip is sharp enough to act as a sufficiently good yet small disturber of the refractive index and to tunnel the evanescent light away from the cladding surface.

In order to confirm the near-field nature of the signal and to estimate the far field contribution NSOM measurements were regularly performed with the feed-back turned off, thus removing the probe from the surface. Usually, the far field contribution did not exceed 10% of the total measured near-field signal. Additionally, the loss of the lateral resolution in NSOM measurements was an indication that the experimental conditions (most often condition of the probe) no longer allowed measuring the near-field signal correctly. In such case the probe was inspected and if necessary replaced. As a rule, at least three independent measurements with different probes were performed with each sample before drawing any conclusions.

**Bare fiber imaging.** The pattern of near field light distribution on the surface of bare TFBG (Fig. 3) qualitatively resembles that of the far field (Fig. 2B): stripes of high and low intensity can be observed perpendicular to the TFBG axis. At the same time, in addition to the 1 micrometer period observed in the far field, some fine structure can be resolved in the stripes with the smallest feature detected on the order of 150 nm (Fig. 3 inset B) and a period of  $\sim 220$  nm (Fig. 3 inset A). The near-field nature of this fine structure is confirmed by its disappearance when the NSOM probe is withdrawn from the surface (feedback is turned off), or is damaged or contaminated. The origin of the shorter period pattern in the near field is attributed to a standing-wave interference between counter-propagating guided cladding modes, including those arising from the back propagating light

reflected by a gold mirror reflector located downstream from the TFBG.<sup>26,27</sup>

**Nanocube coating modifications of the NSOM pattern.** The comparison of the near field pattern between a bare TFBG and one coated with silver nanocubes (shown on Fig. 4 with the same colour mapping of the measured intensity for the two cases) shows a similar trend as the far field images: the regular pattern on the bare fiber (Fig. 4A) becomes an irregular speckle pattern on the coated fiber (Fig. 4B). The minimum size of the speckles observed is likely limited by the spatial resolution of the NSOM probe to about 150 nm. Nevertheless it is obvious that not only is the signal modified laterally but also the intensity of the NSOM images is significantly greater for the coated plasmonic TFBG. On average an enhancement of one order of magnitude is observed ( $2.76$  vs.  $37.3$  mV signal detected by photomultiplier tube).

Dispersed in the images, occasional bright (hot) spots are seen with an instrument-limited lateral dimension of about 150 nm and about two orders of magnitude greater than the average bare fiber signal. The significantly enhanced near field in deep sub-wavelength sized regions of the coated TFBG compared to the bare fiber provides experimental evidence to support our previously suggested hypothesis for the origin of the enhanced light-matter interactions at the surface of plasmonic fiber devices.

The laser wavelength of 647 nm used in our measurements can excite hybrid dipolar resonance only<sup>22</sup> and as such the observed enhancement of light at the TFBG surface can be mediated by this resonance. Theoretical calculations performed using finite element<sup>19</sup> or finite difference time domain<sup>28</sup> methods predicted enhancement of electric field near the top facet of such supported nanocubic structure for the D mode to be around 5–10 times. This level of electric field enhancement is of the same order as our observations of 10–60 times enhanced light at the fiber surface (Fig. 4).

The conclusion that this is a silver nanocube plasmon mediated process is also confirmed by experiments with

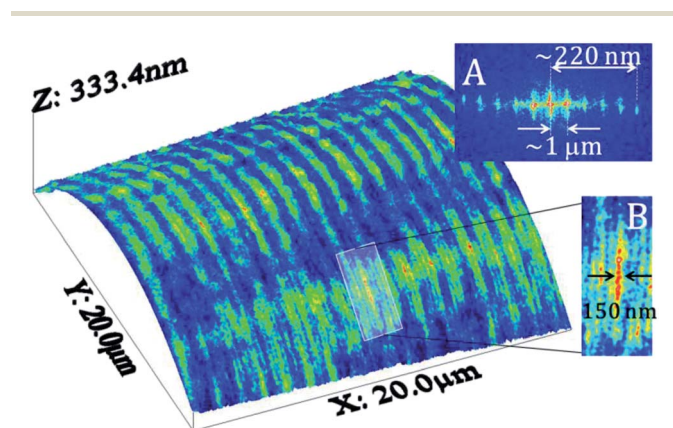


Fig. 3 Typical NSOM image obtained for a bare TFBG overlaid with the fiber topography. Stripes of varying intensity perpendicular to the TFBG axis can be observed. Inset (A) shows a fast Fourier transform of the image with corresponding shortest period of the stripes of  $\sim 220$  nm and the longest period of  $\sim 1$  micrometer. Inset (B) shows the typical optical resolution of 150 nm of the NSOM system.

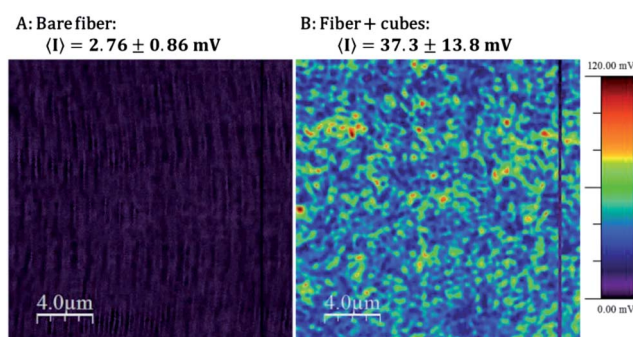


Fig. 4 Typical NSOM images of a bare (A) and coated with nanocubes (B) areas of the same TFBG obtained in the same set of experiments with the same NSOM probe. Laser light was temporarily blocked (dark vertical stripes) to determine the optical signal zero intensity. Average intensities of the optical signal are indicated at the top. About 13 times enhancement on average was observed from the area of the TFBG coated with nanocubes. A maximum signal enhancement of  $\sim 60$  times was observed.

nanoparticles of different sizes and therefore lacking plasmonic signatures at the excitation wavelength (647 nm in our experiments). For instance, 1–5  $\mu\text{m}$ -long silver nanorods showed no detectable near-field enhancement and sometimes even signal attenuation.

**Polarization dependence.** Finally, the spatial distribution and intensity of the bright spots on the surface of the plasmonic

TFBG were found to depend on the polarization of the input excitation light and on the location relative to nanocube agglomerates. The Fig. 5 images show such dependence for four different polarization states. More detailed results are presented as ESI.†

The images overlay the near field signal over the topography. It is clear that the optical pattern changes with changing the

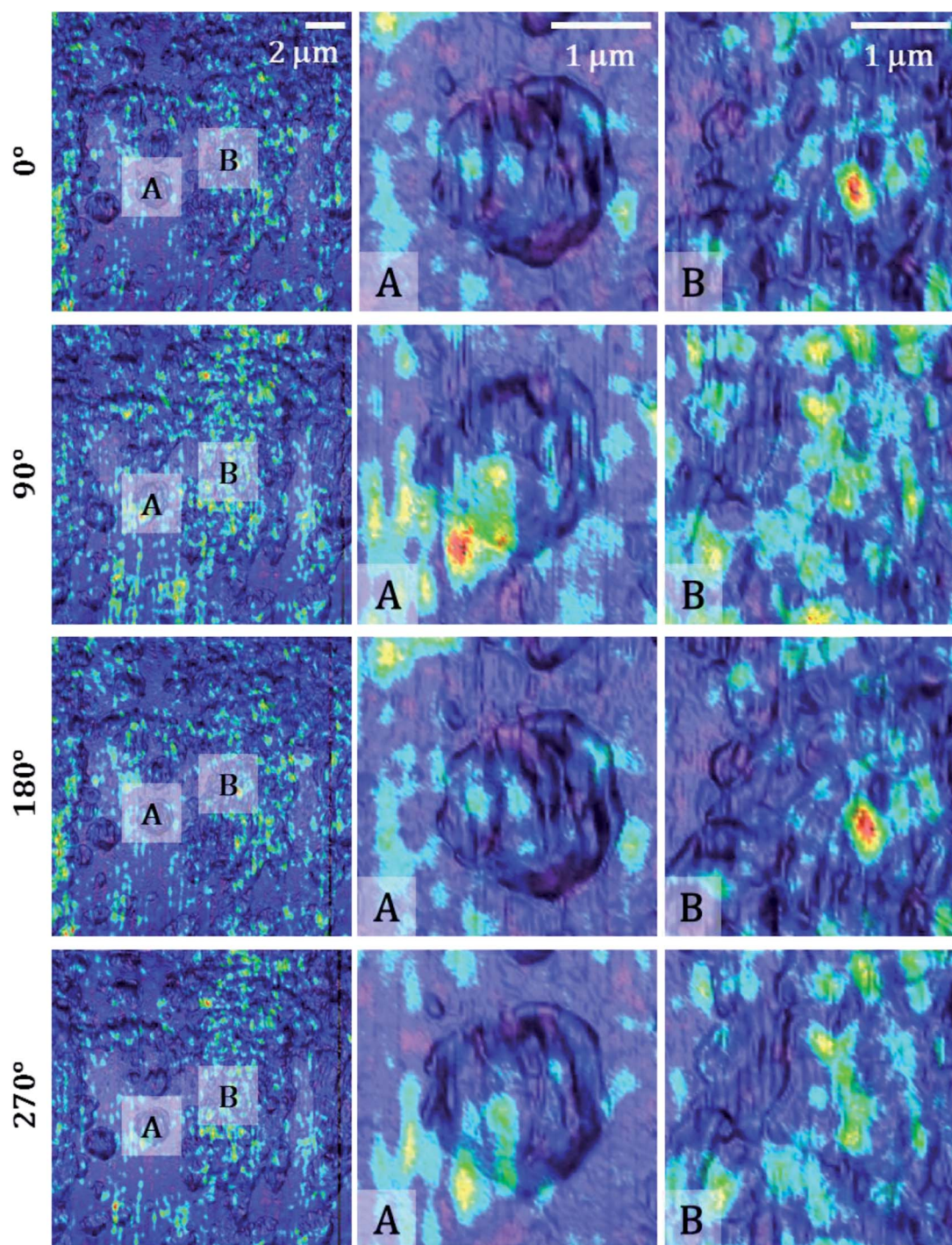


Fig. 5 Polarization dependence of the NSOM signal on the TFBG with randomly deposited nanocubes. Optical  $15 \times 15 \mu\text{m}^2$  images (left column) overlay the topography. Two  $3 \times 3 \mu\text{m}^2$  areas (A and B) were selected to demonstrate a 180 degrees periodicity in the position and intensity of characteristic features. Detailed NSOM images for 12 different polarizations are presented in ESI.†

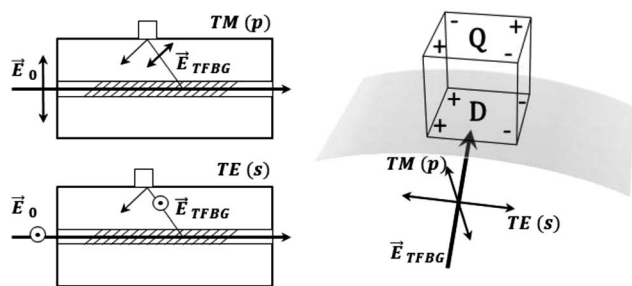


Fig. 6 Dependence of cladding modes polarization on the relative orientation of the entrance beam electric field vector and the Bragg grating tilt plane (left). Schematic showing charge distribution for supported silver nanocube hybrid dipolar (D) and quadrupolar (Q) resonances and relative orientation of TM and TE polarized modes (right).

polarization and repeats itself after a 180 degrees rotation. Slight differences in the images taken at 180 degrees of each other reflect the level of reproducibility of the NSOM over successive scans, as the input light intensity was not changed during the experiments. It is also worth noting that these bright spots are always located near nanocubes seen as irregular domains in the topography images due to the limited topography resolution of the NSOM. Such polarization dependence and location near particular topographic features further confirm the plasmonic nature of the signal enhancement as the excitation of plasmonic resonances responsible for those hot spots is strongly dependent on polarization.<sup>18,29,30</sup>

The relationship between the input light polarization and the orientation of the electric field of the evanescent mode is described in Fig. 6. When core-guided light is incident on a TFBG with a linear polarization aligned in the plane of the tilt (p-polarized or TM) it couples to predominantly radially polarized cladding modes while s-polarized (TE) light incidence results in azimuthally polarized cladding modes.<sup>9,15</sup> Therefore, on the scale of the nanocubes and the wavelength, TE light is polarized in the plane of the nanocube substrate support while TM light is polarized perpendicular to that plane.

Hybrid plasmonic D and Q resonances excited in supported silver nanocubes correspond to oscillations of electrons at the facets close to (D) and away from (Q) the substrate (Fig. 6, right).<sup>21</sup> In addition, we recently demonstrated strong polarization dependence of these modes.<sup>29</sup> Therefore, the orthogonal response shown in Fig. 5 results most likely from excitation of the different plasmonic resonances by TE and TM light sources. In particular, hotspots occur at different locations for the two orthogonal polarization states and reflect different local arrangements of the randomly distributed nanocubes.

The relatively low enhancement factors observed of “only” two orders of magnitude can be rationalized by several factors. On one hand, the NSOM probe must not approach the nanocubes too closely, in order to prevent any nanocube layer or probe damage and as such does not measure the strongest light intensity. On the other, the main field enhancement predicted for the nanocube structure at the wavelength used here should be at the nanocube/fiber interface,<sup>19</sup> *i.e.* hidden from view by the

NSOM (but still available to help increase sensitivity or nonlinear processes), especially since the dipolar resonance excited by the most intense part of the cladding mode evanescent fields is associated primarily with the charge oscillations at the nanocube/fiber facet. However, the fields that were observed occurred at the top of individual or aggregates of nanocubes oriented randomly. It is likely that much stronger field enhancement and therefore extraction from the fiber takes place between pairs of nanocubes at the nanocube/fiber interface which unfortunately cannot be measured using this approach. While it is likely that precisely ordered arrays of identical nanocubes could yield higher enhancement factors, this would require much greater fabrication cost and difficulty, especially on the highly curved surface of an optical fiber. Nevertheless, the localized enhancement of the evanescent optical field of guided modes on the surface of a plasmonic TFBG was demonstrated and provides evidence for the enhanced performance of sensing devices based on such structures.

## Experimental

### Tilted fiber Bragg grating (TFBG)

The uniform, 1 cm-long TFBG with a tilt angle of 10° and period of 556 nm are inscribed in the core of a standard single mode telecommunications optical fibre (CORNING SMF-28) in less than two minutes of irradiation at 248 nm and 100 pulses per s (approximately 40 mJ cm<sup>-2</sup> per pulse) from a pulsed KrF excimer laser in fibers that had been hydrogen-loaded at 2500 psi for about 10 days to enhance their photosensitivity.<sup>9</sup> A phase mask was used to generate a periodic, permanent refractive index pattern in the fibre core.<sup>9</sup>

### Deposition of nanocubes on TFBG

The bare TFBG was cut ~1 cm from the end of the grating and then submerged in piranha solution (H<sub>2</sub>SO<sub>4</sub>/H<sub>2</sub>O<sub>2</sub>) for 20 minutes followed by a 1% (v/v) solution of 3-aminopropyltrimethoxysilane in methanol for an additional 20 minutes. The fiber was then left in the solution of silver nanocubes (synthesized according to the procedure reported previously<sup>31</sup>) with only half of the grating immersed for 1–24 hours, the duration depending on the desired density. After the immersion, the TFBG was rinsed in methanol, and dried under a stream of nitrogen. A 200 nm thick gold coating was deposited on the cleaved end by electroless plating<sup>20</sup> to form a reflecting mirror. The mirror eliminates light scattering from the free fiber end and increases the amount of light incident on the grating. The fiber was secured onto a glass slide, centered on the TFBG, and positioned for NSOM measurements.

### Near-field scanning optical microscopy

NSOM measurements were performed in collection mode using the Ntegra (NTMDT, Russia) scanning probe platform with a 50 × 50 μm<sup>2</sup> scanner. NSOM probes were prepared from high GeO<sub>2</sub>-doped single mode optical fiber (Mitsubishi Cable Industries SSP5155, 5 μm core diameter, 125 μm cladding, 1.45

$\mu\text{m}$  cut-off wavelength) by using the buffered oxide etching method.<sup>24</sup> Light and scanning electron microscopy images were used to monitor the formation of the probes with length of  $3.83 \pm 0.24 \mu\text{m}$  on average. The fabricated uncoated fiber probe was glued along one of the prongs of a tuning fork designed for the use in the instrument. The resonance frequency of the probes was around 190 kHz and the quality factor 400–500. The distance control relied on the damping of the tuning fork oscillations amplitude. The set point for the measurements was chosen at 90–95% of the free probe amplitude to provide reproducible imaging without damaging the sample or the probe. The near-field signal collected by the NSOM probe was measured at the opposite end of the fiber with a Hamamatsu photomultiplier tube (PMT). NSOM and corresponding topography images were collected simultaneously by scanning the TFBG attached to a glass slide with light from a continuous wave mixed gas ion laser (Coherent, Innova 70 Spectrum) coupled into TFBG. A half-wave plate was used to rotate the linear polarization state of the input laser light relative to the tilt plane direction of the grating. Typically  $20 \times 20 \mu\text{m}^2$  images were recorded using scanning frequencies between 0.1–0.5 Hz, and  $512 \times 512$  or  $1024 \times 1024$  points per image. The direction and the origin of scans were varied to check for any possible artifacts. Optical and topography resolutions were estimated by using the full width at half maximum for the smallest features in one of its respective scans. Loss of the optical or topography resolution was used as an indicator of probe contamination or damage. Images were processed with Nova and WSxM software. Conclusions made in this work are based on results of several independent experimental series with at least three different TFBG samples and at least five NSOM probes.

## Conclusions

In the present work, we experimentally measured the polarization selective enhancement by two orders of magnitude of the near-field of optical fiber cladding modes. The enhancement results from plasmonic properties of silver nanocubes and explains the enhanced performance of plasmonic fiber based devices reported previously.

## Acknowledgements

Financial support was provided by NSERC. We thank Adam Bottomley for providing silver nanocube samples and J. Wang for help with SEM and TEM imaging.

## References

- 1 M. Moskovits, *J. Raman Spectrosc.*, 2005, **36**, 485.
- 2 J. R. Lakowicz, *Anal. Biochem.*, 2001, **298**, 1.
- 3 H. A. Atwater and A. Polman, *Nat. Mater.*, 2010, **9**, 205.
- 4 K. Awazu, M. Fujimaki, C. Rockstuhl, J. Tominaga, H. Murakami, Y. Ohki, N. Yoshida and T. Watanabe, *J. Am. Chem. Soc.*, 2008, **130**, 1676.
- 5 S. Mukherjee, F. Libisch, N. Large, O. Neumann, L. V. Brown, J. Cheng, J. B. Lassiter, E. A. Carter, P. Nordlander and N. J. Halas, *Nano Lett.*, 2013, **13**, 240.
- 6 P. Zijlstra, P. M. R. Paulo and M. Orrit, *Nat. Nanotechnol.*, 2012, **7**, 379.
- 7 I. Ament, J. Prasad, A. Henkel, S. Schmachtel and C. Sönnichsen, *Nano Lett.*, 2012, **12**, 1092.
- 8 A. Ahmed and R. Gordon, *Nano Lett.*, 2012, **12**, 2625.
- 9 J. Albert, L.-Y. Shao and C. Coucheteur, *Laser Photonics Rev.*, 2013, **7**, 83.
- 10 I. Del Villar, I. R. Matías and F. J. Arregui, *Opt. Express*, 2005, **13**, 56.
- 11 J. M. Renoirt, C. Zhang, M. Debliqy, M.-G. Olivier, P. Megret and C. Cauchetur, *Opt. Express*, 2013, **21**, 29073.
- 12 A. Bialiaieu, A. Bottomley, D. Prezgot, A. Ianoul and J. Albert, *Nanotechnology*, 2012, **23**, 444012.
- 13 S. Lepinay, A. Staff, A. Ianoul and J. Albert, *Biosens. Bioelectron.*, 2014, **52**, 337.
- 14 D. L. Stokes and T. Vo-Dinh, *Sens. Actuators, B*, 2000, **69**, 28.
- 15 M. Z. Alam and J. Albert, *J. Lightwave Technol.*, 2013, **31**, 3167.
- 16 A. G. Simpson, K. Zhou, L. Zhang, L. Overall and I. Bennion, *Appl. Opt.*, 2004, **43**, 33.
- 17 G. Meltz and W. W. Morey, *Optical Fiber Communication Conference*, 1991, TuM2.
- 18 P. Albella, B. Garcia-Cueto, F. Gonzalez, F. Moreno, P. C. Wu, T.-H. Kim, A. Brown, Y. Yang, H. O. Everitt and G. Videen, *Nano Lett.*, 2011, **11**, 3531.
- 19 S. Zhang, K. Bao, N. J. Halas, H. Xu and P. Nordlander, *Nano Lett.*, 2011, **11**, 1657.
- 20 A. Bialiaieu, C. Cauchetur, N. Ahamad, A. Ianoul and J. Albert, *Opt. Express*, 2011, **19**, 18742.
- 21 K. Tarnowski and W. Urbanczyk, *Opt. Express*, 2013, **21**, 21800.
- 22 A. Bottomley, D. Prezgot, A. Staff and A. Ianoul, *Nanoscale*, 2012, **4**, 6374.
- 23 R. C. Reddick, R. J. Warmack and T. L. Ferrell, *Phys. Rev. B: Condens. Matter Mater. Phys.*, 1989, **39**, 767.
- 24 P. Burgos, Z. Lu, A. Ianoul, C. Hnatovsky, M. L. Viriot, L. Johnston and R. S. Taylor, *J. Microsc.*, 2003, **211**, 37.
- 25 tA. Ianoul, D. D. Grant, Y. Rouleau, M. Bani-Yaghoub, L. J. Johnston and J. P. Pezacki, *Nat. Chem. Biol.*, 2005, **1**, 196.
- 26 J. D. Mills, C. W. J. Hillman and W. S. Brocklesby, *Appl. Phys. Lett.*, 1999, **75**, 4058.
- 27 A. J. Meixner, M. A. Bopp and G. Tarach, *Appl. Opt.*, 1994, **33**, 7995.
- 28 L. J. Sherry, S.-H. Chang, G. C. Schatz, R. P. Van Duyne, B. J. Wiley and Y. Xia, *Nano Lett.*, 2005, **5**, 2034.
- 29 J. Jiang, K. Bosnick, M. Maillard and L. Brus, *J. Phys. Chem. B*, 2003, **107**, 9964.
- 30 J. M. McLellan, Z.-Y. Li, A. R. Siekkinen and Y. Xia, *Nano Lett.*, 2007, **7**, 1013.
- 31 N. Ahamad, A. Bottomley and A. Ianoul, *J. Phys. Chem. C*, 2012, **116**, 185.